

AI-Driven Design of Stacked Intelligent Metasurfaces for Software-Defined Radio Applications

Ivan Iudice
Security Unit
Italian Aerospace Research Centre
(CIRA)
Capua I-81043
i.iudice@cira.it

Giacinto Gelli
Dept. of Electrical Engineering
and Information Technology
University of Naples Federico II
Naples I-80125
gelli@unina.it

Donatella Darsena
Dept. of Electrical Engineering
and Information Technology
University of Naples Federico II
Naples I-80125
darsena@unina.it

Abstract— The integration of reconfigurable intelligent surfaces (RIS) into future wireless communication systems offers promising capabilities in dynamic environment shaping and spectrum efficiency. In this work, we present a consistent implementation of a stacked intelligent metasurface (SIM) model within the NVIDIA’s AI-native framework Sionna for 6G physical layer research. Our implementation allows simulation and learning-based optimization of SIM-assisted communication channels in fully differentiable and GPU-accelerated environments, enabling end-to-end training for cognitive and software-defined radio (SDR) applications. We describe the architecture of the SIM model, including its integration into the TensorFlow-based pipeline, and showcase its use in closed-loop learning scenarios involving adaptive beamforming and dynamic reconfiguration. Benchmarking results are provided for various deployment scenarios, highlighting the model’s effectiveness in enabling intelligent control and signal enhancement in non-terrestrial-network (NTN) propagation environments. This work demonstrates a scalable, modular approach for incorporating intelligent metasurfaces into modern AI-accelerated SDR systems and paves the way for future hardware-in-the-loop experiments.

efficiency through programmable manipulation of incident electromagnetic (EM) waves [2–4].

Beyond the substantial progress made in RIS research, recent studies have investigated multi-layer and dynamic implementations, so called *stacked intelligent metasurfaces* (SIMs), to further increase the available degrees-of-freedom (DoF). Inspired by diffractive optical platforms, SIMs are realized as cascades of programmable metasurfaces, each endowed with adaptive or intelligent control capabilities [5–8]. SIMs can implement signal-processing transformations directly in the EM wave domain, generating tailored wave profiles as the input propagates through the layers. Their integration into wireless systems can replace conventional digital beamforming architectures, reducing the need for high-resolution DACs/ADCs and minimizing the number of RF chains, thereby lowering hardware costs and power consumption. Moreover, since multi-antenna precoding and combining occur directly in the wave domain at the speed of light, SIM architectures mitigate processing delays of digital solutions.

To the best of our knowledge, despite these advances, existing studies rarely consider key aspects such as scalability, differentiability, and integration into AI-native physical-layer pipelines. Moreover, only limited attention has been given in the metasurface literature to programmable NTN scenarios or GPU-accelerated architectures suitable for closed-loop learning. These gaps motivate the development of a framework aimed at enabling scalable simulation and optimization of multi-layer programmable surfaces in realistic NTN contexts.

To this end, we propose the first consistent integration of a SIM model within NVIDIA’s AI-native framework *Sionna*. Sionna is a GPU-accelerated, fully differentiable library for communication system simulation and optimization, built on TensorFlow and designed for rapid prototyping and end-to-end learning in next-generation wireless systems [9, 10]. Our SIM implementation extends Sionna’s modular architecture, enabling efficient simulation and gradient-based optimization of SIM-assisted channels in both terrestrial and NTN environments.

The main contributions of this paper are summarized as follows:

- We develop a mathematically grounded and differentiable model of SIM, designed for seamless integration into Sionna’s TensorFlow-based simulation pipeline.
- We demonstrate efficient GPU-accelerated simulation and optimization of SIM, exploiting Sionna’s end-to-end gradient propagation and modular design.
- We apply our framework to a closed-loop learning scenario, exemplified by adaptive beamforming.

Sixth-generation (6G) wireless communication systems are expected to dramatically outperform previous generations by leveraging AI-native technologies, the *non-terrestrial network* (NTN) paradigm, software-defined radio architectures, and programmable radio environments [1]. A particularly promising approach in this context is that of *reconfigurable intelligent surfaces* (RIS), which enable the realization of *software-defined environments* by dynamically shaping the propagation medium and enhancing spectrum and energy

We validate the proposed framework through numerical benchmarks, comparing SIM-enabled systems with conventional multi-antenna baselines. The obtained results highlight significant improvements in spectral efficiency and signal fidelity. Overall, this work establishes a scalable foundation for integrating intelligent metasurfaces into AI-driven SDR systems and paves the way towards hardware-in-the-loop experimentation and real-world deployment.

The remainder of the paper is organized as follows. Section 2 reviews related work on RIS and differentiable simulation frameworks. Section 3 introduces the mathematical model of stacked intelligent metasurfaces, while Section 4 describes the model-based optimization. Section 5 details the implementation within Sionna. Section 6 presents learning-based optimization and performance benchmarks. Section 7 concludes the paper, discussing future research directions.

2. BACKGROUND AND RELATED WORK

Reconfigurable intelligent surfaces (RISs), also referred to as *intelligent reflecting surfaces* (IRSs), have recently emerged as a fundamental paradigm for future 6G networks, providing the basis for programmable wireless environments [11, 12]. Composed of tunable sub-wavelength elements, RIS can manipulate incident EM waves by dynamically adjusting their reflection, refraction, or absorption characteristics. Compared to conventional active relays, they offer low-power operation and scalable deployment, and have been widely studied for many applications, such as energy-efficient communications, beamforming, secure transmission, and localization [2, 13, 14]. Moreover, RIS are receiving increasing attention in non-terrestrial networks (NTN), where satellite and aerial platforms can benefit from enhanced channel programmability [4].

Beyond traditional single-layer designs, the concept of *stacked intelligent metasurfaces* (SIMs) introduces multiple programmable layers with adaptive or intelligent capabilities [15]. Such architectures enable richer channel transformations, finer waveform control, and improved robustness against hardware constraints. By operating directly in the EM domain, SIMs can implement signal processing transformations in the wave itself, tailoring the input as it propagates through the layers to produce a desired output profile. This approach opens the way to replacing conventional digital beamforming structures, thereby reducing the need for high-resolution DACs/ADCs and minimizing the number of RF chains, with consequent savings in hardware cost and power consumption. Furthermore, multi-antenna precoding and combining are inherently performed in the wave domain as the signal propagates at the speed of light, reducing processing delay in comparison to purely digital solutions.

Despite these promising features, the integration of SIMs into differentiable, AI-native simulation frameworks remains largely unexplored. In parallel, the rise of AI-driven physical-layer research has motivated the development of differentiable, GPU-accelerated simulators. Among them, NVIDIA’s *Sionna* library has been introduced as a modular TensorFlow-based platform supporting automatic differentiation, end-to-end learning, and rapid prototyping [9], while its recent extension *Sionna RT* incorporates differentiable ray tracing for realistic propagation modeling in dynamic environments [16]. Nevertheless, no scalable multi-layer SIM model has yet been integrated into Sionna, thus leaving an open gap for the simulation and optimization of intelligent metasurfaces in

software-defined radio (SDR) and NTN scenarios.

3. SYSTEM MODEL

We consider the SIM-aided downlink communication system illustrated in Fig. 1. In this setup, a satellite (SAT) is equipped with N antennas and employs a SIM consisting of L planar metasurface layers to communicate with K single-antenna user equipments (UEs). Let s denote the spacing between two adjacent layers of the SIM, and σ the distance between the array and the first layer of the SIM. The ℓ -th layer of the SIM is composed of $Q^{(\ell)} \triangleq Q_x^{(\ell)} \times Q_y^{(\ell)}$ meta-atoms arranged in a rectangular grid, with $Q_x^{(\ell)}$ and $Q_y^{(\ell)}$ elements along the x and y axes, respectively, and a constant inter-element spacing d_{RIS} . For simplicity, we introduce a mapping that converts the 2-D index (q_x, q_y) of a meta-atom in the ℓ -th layer, where $q_x \in \{0, 1, \dots, Q_x^{(\ell)} - 1\}$ and $q_y \in \{0, 1, \dots, Q_y^{(\ell)} - 1\}$, into a one-dimensional (1-D) index $q \triangleq q_x Q_y^{(\ell)} + q_y$ belonging to $\mathcal{Q}^{(\ell)} \triangleq \{0, 1, \dots, Q^{(\ell)} - 1\}$. This mapping indexes the meta-atoms sequentially from row to row within each layer. It should be noted that, within this architecture, each layer can be designed with a different number of meta-atoms, allowing flexibility in the overall metasurface configuration.

In this work, we adopt the well-established analytical propagation model proposed in [5–8, 17–22]. Specifically, each metasurface layer is assumed to be perfectly impedance-matched, thereby eliminating backward reflections and focusing exclusively on forward propagation. When an incident EM wave with carrier frequency $f_0 > 0$ impinges on a meta-atom of the first layer, the amplitude and phase of the transmitted wave are determined by the product of the incident electric field and the complex transmission coefficient of that meta-atom. The resulting transmitted wave acts as a secondary source that illuminates all meta-atoms of the subsequent layer, in accordance with the Huygens–Fresnel principle [23].

Furthermore, to enhance the degrees-of-control (DoC) in the wave-domain transformation performed by the SIM, we consider the model architecture proposed in [24], incorporating both *amplitude-controlled* (AC) and *phase-controlled* (PC) layers into the stacked device [24]. Specifically, PC layers are nearly passive, allowing only phase adjustments of their meta-atoms via components such as varactor or PIN diodes. In contrast, AC layers are active and enable amplitude modulation of their meta-atoms through the integration of amplifier chips. This combination of PC and AC layers in the SIM facilitates independent manipulation of amplitude and phase in the wave domain.

Let $\tau_{\ell,q} = \alpha_{\ell,q} e^{j\phi_{\ell,q}}$ represent the EM transmission coefficient of the q -th meta-atom in the ℓ -th metasurface layer, with $\ell \in \mathcal{L} \triangleq \{1, 2, \dots, L\}$ and $q \in \mathcal{Q}^{(\ell)}$. We define \mathcal{L}_{ac} and \mathcal{L}_{pc} as two nonoverlapping subsets of \mathcal{L} that index the AC and PC layers, respectively, whose cardinalities L_{ac} and L_{pc} satisfy the condition $L_{\text{ac}} + L_{\text{pc}} = L$. The transmission coefficients for each layer of the SIM are organized into diagonal matrices $\mathbf{T}_\ell \triangleq \text{diag}(\boldsymbol{\tau}_\ell) \in \mathbb{C}^{Q^{(\ell)} \times Q^{(\ell)}}$, where $\boldsymbol{\tau}_\ell \triangleq [\tau_{\ell,0}, \tau_{\ell,1}, \dots, \tau_{\ell,Q^{(\ell)}-1}]$ and $\ell \in \mathcal{L}$. AC layers consist of meta-atoms whose amplitude responses $\{\alpha_{\ell,q}\}_{\ell \in \mathcal{L}_{\text{ac}}}$ can be independently controlled through software. The phases $\{\phi_{\ell,q}\}_{\ell \in \mathcal{L}_{\text{ac}}}$ of the transmission coefficients in AC layers are fixed and cannot be adjusted. Consequently, these phases

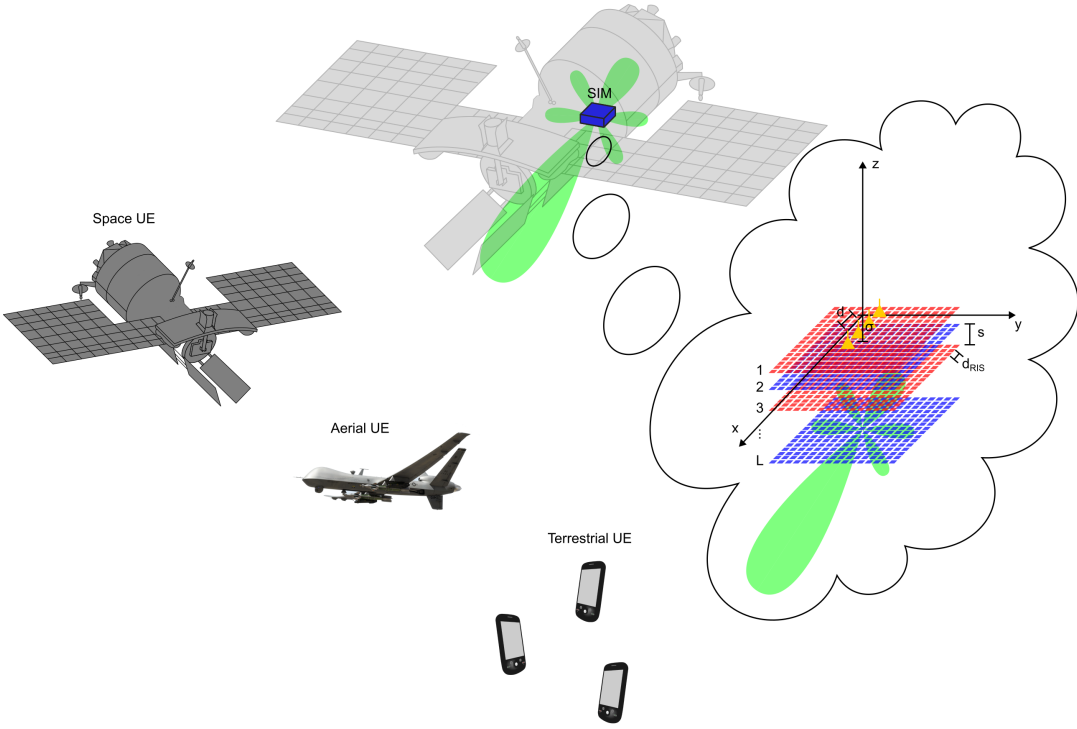


Figure 1. SIM-aided downlink architecture with amplitude-controlled (red) and phase-controlled (blue) layers.

will be treated as known but uncontrollable in the subsequent optimization process. For PC layers, the metasurfaces are locally passive, i.e., their meta-atoms cannot amplify the incident EM waves. Due to the unavoidable material losses, PC layers may attenuate the EM waves that penetrate through them, implying that their amplitude responses are generally smaller than one, i.e., $\alpha_{\ell,q} \leq 1$ for $\ell \in \mathcal{L}_{\text{pc}}$. Therefore, we assume that the PC layers have a constant transmittance, meaning that the amplitude responses are fixed at $\alpha_{\ell,q} = \alpha_{\text{pc}} \leq 1$ for $\ell \in \mathcal{L}_{\text{pc}}$. The phases $\{\phi_{\ell,q}\}_{\ell \in \mathcal{L}_{\text{pc}}}$ can be adjusted within the interval $[0, 2\pi]$.

The channel coefficients between the N transmit antennas of the SAT array and the $Q^{(1)}$ meta-atoms of the first layer of the SIM are organized into the matrix $\mathbf{W}_1 \in \mathbb{C}^{N \times Q^{(1)}}$. These coefficients are modeled using *Rayleigh-Sommerfeld diffraction theory* as follows

$$\{\mathbf{W}_1\}_{n,q} = \frac{A_{\text{bs}} \cos(\theta_{n,q}^{(1)})}{d_{n,q}^{(1)}} \left(\frac{1}{2\pi d_{n,q}^{(1)}} - \frac{j}{\lambda_0} \right) e^{j \frac{2\pi}{\lambda_0} d_{n,q}^{(1)}} \quad (1)$$

for $n \in \mathcal{N} \triangleq \{0, 1, \dots, N-1\}$ and $q \in \mathcal{Q}^{(1)}$, where $\lambda_0 = c/f_0$ is the wavelength, with $c = 3 \cdot 10^8$ m/s denoting the light speed in vacuum, A_{bs} is the effective area of the antennas of the array (evaluated at f_0), $\cos(\theta_{n,q}^{(1)}) = \sigma/d_{n,q}^{(1)}$, and $d_{n,q}^{(1)}$ denotes the distance between the n -th antenna of the SAT and the q -th meta-atom of the first layer. This distance reads as

$$d_{n,1}^{(1)} = \sqrt{\left(x_q^{(1)} - x_n^{(0)}\right)^2 + \left(y_q^{(1)} - y_n^{(0)}\right)^2 + \sigma^2} \quad (2)$$

with $(x_q^{(1)}, y_q^{(1)})$ and $(x_n^{(0)}, y_n^{(0)})$ representing the 2-D coordinates of the q -th meta-atom on the first layer of the SIM and the position of the n -th antenna of the SAT, respectively.

Similarly, for each $\ell \in \mathcal{L} - \{1\}$, the forward propagation process between layers $\ell-1$ and ℓ is described by the matrix $\mathbf{W}_\ell \in \mathbb{C}^{Q^{(\ell-1)} \times Q^{(\ell)}}$, whose entry $\{\mathbf{W}_\ell\}_{\tilde{q},q}$, for $\tilde{q} \in \mathcal{Q}^{(\ell-1)}$ and $q \in \mathcal{Q}^{(\ell)}$, represents the channel coefficient from the \tilde{q} -th meta-atom in the $(\ell-1)$ -th layer to the q -th meta-atom in the ℓ -th layer, and is given by

$$\{\mathbf{W}_\ell\}_{\tilde{q},q} = \frac{A_{\text{meta}} \cos(\theta_{\tilde{q},q}^{(\ell)})}{d_{\tilde{q},q}^{(\ell)}} \left(\frac{1}{2\pi d_{\tilde{q},q}^{(\ell)}} - \frac{j}{\lambda_0} \right) e^{j \frac{2\pi}{\lambda_0} d_{\tilde{q},q}^{(\ell)}} \quad (3)$$

where A_{meta} is the physical area of the meta-atoms, $\cos(\theta_{\tilde{q},q}^{(\ell)}) = s/d_{\tilde{q},q}^{(\ell)}$, and $d_{\tilde{q},q}^{(\ell)}$ represents the propagation distance between the \tilde{q} -th meta-atom of the $(\ell-1)$ -th layer and the q -th meta-atom of the ℓ -th layer. This distance is given by the following expression

$$d_{\tilde{q},q}^{(\ell)} = \sqrt{\left(x_q^{(\ell)} - x_{\tilde{q}}^{(\ell-1)}\right)^2 + \left(y_q^{(\ell)} - y_{\tilde{q}}^{(\ell-1)}\right)^2 + s^2} \quad (4)$$

with $(x_q^{(\ell)}, y_q^{(\ell)})$ representing the 2-D coordinates of the q -th meta-atom on the ℓ -th layer of the SIM.

The overall forward propagation through the SIM is described by the matrix

$$\mathbf{G} = \mathbf{W}_1 \mathbf{T}_1 \mathbf{W}_2 \mathbf{T}_2 \cdots \mathbf{W}_{L-1} \mathbf{T}_{L-1} \mathbf{W}_L \mathbf{T}_L \in \mathbb{C}^{N \times Q^{(L)}}. \quad (5)$$

For the sake of simplicity, we assume that the SAT employs for transmission a linear modulation format. In particular, let $\{b_k[i]\}_{i \in \mathbb{Z}}$ represent the data stream to be transmitted to the k -th UE, for $k \in \{0, 1, \dots, K-1\}$, the complex envelope

of the narrowband continuous-time signal associated with the k -th data stream is given by

$$s_k(t) = \sum_{i=-\infty}^{+\infty} b_k(i) \psi(t - i T_s). \quad (6)$$

where $\{b_k(i)\}_{k=0}^{K-1}$ are mutually independent sequences of zero-mean unit-variance independent and identically-distributed (i.i.d.) complex random variables. These sequences are transmitted at symbol rate $1/T_s$, with $\psi(t)$ representing the real unit-energy square-root Nyquist pulse-shaping waveform.

Let the vector $\mathbf{x}(t) \triangleq [x_0(t), x_1(t), \dots, x_{N-1}(t)] \in \mathbb{C}^{1 \times N}$ denote the complex envelope of the signal transmitted by the SAT antenna array, which can be written as

$$\mathbf{x}(t) = \sum_{k=0}^{K-1} \mathbf{p}_k s_k(t) = \sum_{i=-\infty}^{+\infty} \sum_{k=0}^{K-1} \mathbf{p}_k b_k(i) \psi(t - i T_s) \quad (7)$$

where $\mathbf{p}_k \in \mathbb{C}^{1 \times N}$ represents the precoding (beamforming) row-vector associated with the k -th data stream. Leveraging the matrix representation one obtains

$$\mathbf{x}(t) = \sum_{i=-\infty}^{+\infty} \mathbf{b}(i) \mathbf{P} \psi(t - i T_s) \quad (8)$$

where $\mathbf{b}(i) \triangleq [b_0(i), b_1(i), \dots, b_{K-1}(i)] \in \mathbb{C}^{1 \times K}$, and $\mathbf{P} \triangleq [\mathbf{p}_0^T, \mathbf{p}_1^T, \dots, \mathbf{p}_{K-1}^T]^T \in \mathbb{C}^{K \times N}$ denotes the precoding matrix.

The baseband signal radiated from the L -th layer of the SIM and propagating through the physical channel admits the following expression:

$$\mathbf{z}(t) = \mathbf{x}(t) \mathbf{G} = \sum_{n=0}^{N-1} x_n(t) \mathbf{g}_n. \quad (9)$$

Using (8) and (9), the total power radiated by the SIM can be expressed as

$$\mathcal{P}_{\text{rad}} \triangleq \langle \mathbb{E}[\|\mathbf{z}(t)\|^2] \rangle = \|\mathbf{P}\mathbf{G}\|_{\text{F}}^2 \leq \mathcal{P}_{\text{S}} \|\mathbf{G}\|^2 \quad (10)$$

where $\mathbb{E}[\cdot]$ represents the ensemble average, $\langle x(t) \rangle \triangleq \lim_{T \rightarrow +\infty} \frac{1}{T} \int_{-T/2}^{T/2} x(t) dt$ is the time average of the continuous-time signal $x(t)$, $\mathcal{P}_{\text{S}} \triangleq \|\mathbf{P}\|_{\text{F}}^2$ is the overall power emitted by the SAT antenna array, with $\|\mathbf{A}\|_{\text{F}}$ denoting the Frobenius norm of the matrix \mathbf{A} , and we have exploited the statistical independence among the information symbols $b_k(i)$.

At the k -th receiver, which is assumed to lie in the far field of the SIM, the waveform is passed through a matched filter with impulse response $\psi(-t)$ and uniformly sampled at the symbol rate $1/T_s$, assuming perfect timing synchronization. The resulting baseband signal $y_k(i) \triangleq y_k(i T_s)$ received by the k -th user during the i -th symbol interval $[i T_s, (i+1) T_s]$, with $k \in \{0, 1, \dots, K-1\}$ and $i \in \mathbb{Z}$, is given by

$$y_k(i) = \mathbf{b}(i) \mathbf{P} \mathbf{G} \mathbf{h}_k^T + r_k(i) \quad (11)$$

where $\mathbf{h}_k \in \mathbb{C}^{1 \times N}$ represents the frequency-flat block-fading channel from the SIM to the k -th user², and $r_k(i)$ denotes (filtered) circularly-symmetric complex Gaussian noise at the k -th user, with zero mean and variance $\mathbb{E}[|r_k(i)|^2] = \sigma_k^2$.

By stacking the received samples of all UEs, we obtain

$$\mathbf{y}(i) = \mathbf{b}(i) \mathbf{P} \mathbf{G} \mathbf{H} + \mathbf{r}(i) \quad (12)$$

where $\mathbf{y}(i) \triangleq [y_0(i), y_1(i), \dots, y_{K-1}(i)] \in \mathbb{C}^{1 \times K}$, $\mathbf{r}(i) \triangleq [r_0(i), r_1(i), \dots, r_{K-1}(i)] \in \mathbb{C}^{1 \times K}$ denotes the noise vector, and $\mathbf{H} \triangleq [\mathbf{h}_0^T, \mathbf{h}_1^T, \dots, \mathbf{h}_{K-1}^T] \in \mathbb{C}^{Q^{(L)} \times K}$ is the channel matrix.

The parameters \mathbf{P} and $\{\tau_{\ell}\}_{\ell \in \mathcal{L}}$ can be tuned by the designer to optimize the communication links.

4. MODEL-BASED OPTIMIZATION

Our aim is to jointly determine the precoding matrix \mathbf{P} and the SIM transmission coefficients $\{\tau_{\ell,q}\}$, for each layer ℓ and meta-atom q , that minimize the following *mean squared error* (MSE):

$$\text{MSE}(\mathbf{P}, \{\tau_{\ell}\}_{\ell \in \mathcal{L}}) \triangleq \mathbb{E}[\|\mathbf{b}(i) - \beta \mathbf{y}(i)\|^2] \quad (13)$$

subject to the transmit power constraint $\|\mathbf{P}\|^2 = \mathcal{P}_{\text{S}}$. By substituting (12) into (13), the optimal solution for the precoding matrix can be expressed as [25]

$$\mathbf{P}_{\text{MMSE}} = \beta^{-1} \mathbf{H}^H \mathbf{G}^H \left(\mathbf{G} \mathbf{H} \mathbf{H}^H \mathbf{G}^H + \frac{1}{\text{SNR}} \mathbf{I}_N \right)^{-1} \quad (14)$$

where the signal-to-noise ratio is defined as

$$\text{SNR} \triangleq \frac{\mathcal{P}_{\text{S}}}{\sum_{k=0}^{K-1} \sigma_k^2} \quad (15)$$

and the normalization factor β is given by

$$\beta = \sqrt{\frac{\text{tr}[\mathbf{H}^H \mathbf{G}^H (\mathbf{G} \mathbf{H} \mathbf{H}^H \mathbf{G}^H + \frac{1}{\text{SNR}} \mathbf{I}_N)^{-2} \mathbf{G} \mathbf{H}]}{\mathcal{P}_{\text{S}}}}. \quad (16)$$

Substituting (14) into (13), we obtain

$$\text{MSE}(\mathbf{P}_{\text{MMSE}}, \{\tau_{\ell}\}_{\ell \in \mathcal{L}}) = K - \text{tr}[\mathbf{H}^H \mathbf{G}^H \left(\mathbf{G} \mathbf{H} \mathbf{H}^H \mathbf{G}^H + \frac{1}{\text{SNR}} \mathbf{I}_N \right)^{-1} \mathbf{G} \mathbf{H}]. \quad (17)$$

By further exploiting the spectral representation of (17), it follows that

$$\text{MSE}(\mathbf{P}_{\text{MMSE}}, \{\tau_{\ell}\}_{\ell \in \mathcal{L}}) = K - \sum_{k=0}^{R_m-1} \frac{\tilde{s}_k^2}{\tilde{s}_k^2 + 1/\text{SNR}} \quad (18)$$

²The considered signal model can be readily adapted to more complicated modulation schemes (e.g., CP-OFDM) possibly adopted to cope with the time-dispersive nature of wireless channels.

where $R_m \triangleq \min(K, \text{rank}(\mathbf{GH}))$, and $\tilde{s}_k \in \mathbb{R}$ denotes the k -th singular value of \mathbf{GH} .

Assuming that \mathbf{H} is full rank, the objective is to design \mathbf{G} so that \mathbf{GH} is also full rank, i.e., $R_m = K$, while maximizing the singular values $\{\tilde{s}_k^2\}_{k=0}^{K-1}$ under constraint (6). This is achieved when the rows of \mathbf{G} are aligned with the left singular vectors of \mathbf{H} .

Specifically, consider the singular value decomposition (SVD) of $\mathbf{H} = \mathbf{U}_H \mathbf{S}_H \mathbf{V}_H^H$, where $\mathbf{U}_H \in \mathbb{C}^{Q^{(L)} \times Q^{(L)}}$ and $\mathbf{V}_H \in \mathbb{C}^{K \times K}$ are unitary matrices, and

$$\mathbf{S}_H \triangleq \begin{bmatrix} s_0 & 0 & \cdots & 0 \\ 0 & s_1 & \cdots & 0 \\ \vdots & \vdots & \ddots & \vdots \\ 0 & 0 & \cdots & s_{K-1} \\ 0 & 0 & \cdots & 0 \\ \vdots & \vdots & \ddots & \vdots \\ 0 & 0 & \cdots & 0 \end{bmatrix} \in \mathbb{R}^{Q^{(L)} \times K}. \quad (19)$$

The SIM can be designed such that $\mathbf{G} = \mathbf{U}_G \mathbf{D} \mathbf{U}_{H,\text{left}}^H$, where $\mathbf{U}_{H,\text{left}} \in \mathbb{C}^{Q^{(L)} \times N}$ collects the first N columns of \mathbf{U}_H , $\mathbf{D} \triangleq \text{diag}(d_0, d_1, \dots, d_{N-1}) \in \mathbb{R}^{N \times N}$, and $\mathbf{U}_G \in \mathbb{C}^{N \times N}$ is unitary [26]. For $N \geq K$, the MSE expression in (18) reduces to

$$\text{MSE}(\mathbf{P}_{\text{MMSE}}, \{\boldsymbol{\tau}_\ell\}_{\ell \in \mathcal{L}}) = K - \sum_{k=0}^{K-1} \frac{d_k^2 s_k^2}{d_k^2 s_k^2 + 1/\text{SNR}}. \quad (20)$$

The optimization problem therefore consists in maximizing the sequence $\{d_k\}_{k=0}^{K-1}$ while satisfying the physical constraints imposed by the SIM architecture. A common simplification is to impose mild, physically motivated constraints such as $\mathbf{G} = \mathbf{U}_{H,\text{left}}^H$ [24], which enforce specific structural properties on the rows of \mathbf{G} .

It is important to note that the model-based approach outlined above assumes perfect knowledge at the SAT of both the overall channel \mathbf{H} and the SNR. In practice, these parameters must be estimated, which not only incurs extra communication overhead but also introduces additional errors in the reception of information.

In the following sections, we propose a learning-based design of both the SIM and the precoder, which exploits modern GPU architectures and the Sionna framework to tackle this optimization problem, while fully exploiting the resources of the SIM.

5. IMPLEMENTATION IN TENSORFLOW

In this section, we describe the implementation of the SIM response and the precoding matrix within the TensorFlow framework. Both have been realized as custom Keras layers [27], making them readily integrable into Sionna or, more generally, into any TensorFlow-based pipeline.

The following provides the implementation of the SIM class.

```
import tensorflow as tf
```

```
...
class SIM(tf.keras.layers.Layer):
    def __init__(self, W_list,
                 mask=None, gain_bounds=None,
                 passive_gain=1.0, seed=None,
                 name="SIM", **kwargs):
...
...
```

As shown, the class takes as input the following arguments: a list W_{list} , which collects the transition matrices defined in (1) and (3); a list mask , specifying for each layer whether it is *active* or *passive*; a list $\text{gain}_\text{bounds}$, defining the amplitude bounds for the active layers; the floating-point value $\text{passive}_\text{gain}$, representing the gain introduced by the passive layers (i.e., α_{pc}); and the integer seed , used to initialize the internal random generator.

The following provides the definition of the `TrainablePrecoder` class.

```
import tensorflow as tf
...
class TrainablePrecoder(tf.keras.layers.Layer):
    def __init__(self, K, N, Ps, init,
                 name="TrainablePrecoder",
                 **kwargs):
...
...
```

As shown, the class takes as input the following arguments: the integers K and N , denoting the number of UEs and the number of antennas, respectively; the floating-point value P_s , representing the total transmit power of the antenna array, i.e., \mathcal{P}_s ; and the $K \times N$ complex matrix init , which specifies the initial values of the precoding matrix.

Both classes have been implemented to be fully differentiable, thereby enabling the exploitation of automatic gradient computation in TensorFlow with GPU acceleration.

6. SIMULATION RESULTS

Monte Carlo simulations were carried out for analyzing the performance of the AI-driven SIM design strategy in comparison with the model-based approach, in terms of *bit-error rate* (BER) versus the energy contrast E_b/N_0 .

Specifically, we considered a SAT equipped with an *uniform planar array* (UPA) composed of $N = 4$ antennas, performing downlink transmission of $K = 4$ information streams to $K = 4$ single-antenna UEs. The UPA antenna spacing is set to $d_s = \lambda_0/2$.

The considered SIM consists of $L = 8$ equally spaced layers with inter-layer spacing $s = \lambda_0/2$, of which $L_{\text{ac}} = 2$ are active layers and $L_{\text{pc}} = 6$ are passive ones. Each layer is formed by $Q = 12 \times 12$ unit cells, arranged with an inter-cell spacing of $s = \lambda_0/2$. The gain of the active unit cells can be tuned between -22 dB and 13 dB, whereas the gain of the passive unit cells is fixed to $\alpha_{\text{pc}} = 0.9$. Quantization effects are not explicitly accounted for, as the proposed solution is applicable to non-reconfigurable architectures as well as to reconfigurable architectures employing meta-atoms that can be controlled in an (almost) continuous manner.

The native `sionna` classes, `BinarySource`, `Mapper`, `Demapper`, and `AWGN` are used for implementing the end-to-end chain.

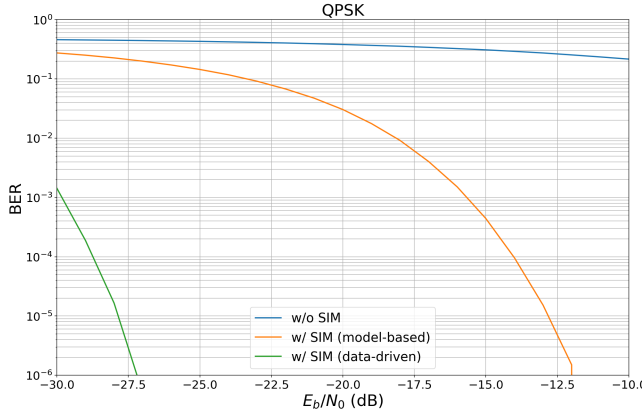


Figure 2. Bit-error rate versus energy contrast for QPSK modulation scheme.

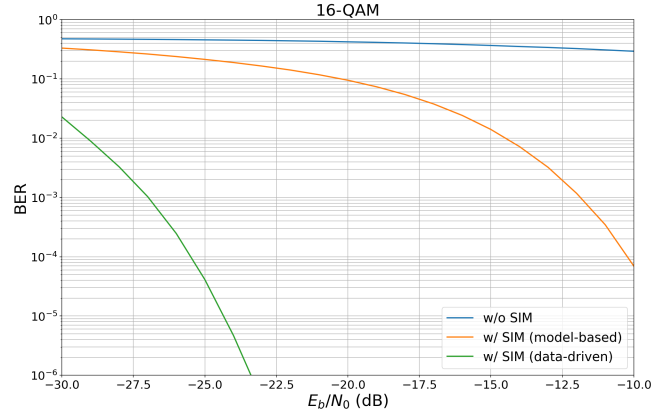


Figure 3. Bit-error rate versus energy contrast for 16-QAM modulation scheme.

For each realization, the entries of the channel matrix \mathbf{H} are generated as i.i.d. circularly symmetric complex Gaussian random variables with zero mean and unit variance. In addition, a block of $N_B = 1000$ bits is generated for each user. For the data-driven approaches, the matrices \mathbf{P} and \mathbf{G} are learned using a block of 100 symbols per realization.

Figures 2 and 3 report the simulation results averaged over $N_{mc} = 1000$ realizations, for QPSK and 16-QAM modulation schemes, respectively. The results clearly indicate that the data-driven approach (green curves) significantly outperforms both its model-based counterpart (orange) and the baseline system without SIM (blue).

At first glance, this behavior may seem counterintuitive; however, it can be explained by the inherent limitations of the adopted SIM model. In particular, the model-based SIM synthesis is obtained by imposing $\mathbf{G} = \mathbf{U}_{\mathbf{H},\text{left}}^H$, which implies $d_k = 1$ for all $k \in \{0, 1, \dots, K-1\}$. This assumption does not allow to fully exploit the array gain that the SIM could provide, especially when active layers are included. Conversely, the data-driven approach is able to exploit the full set of degrees of control offered by the SIM.

When only passive layers are considered, one has $d_k < 1$ for all $k \in \{0, 1, \dots, K-1\}$, and in this case the performance of the data-driven approach deteriorates compared to the model-based design. For brevity, the corresponding simulation results are omitted.

7. CONCLUSION AND FUTURE WORK

This paper introduced a differentiable and GPU-accelerated model for the design and evaluation of SIM integrated within NVIDIA’s Sionna library. By developing a multi-layer SIM model and embedding it into TensorFlow, we enabled end-to-end optimization of both the precoder and the metasurface configuration. Monte Carlo simulations showed that the learning-based design consistently outperforms its model-based counterpart as well as a baseline system without SIM, confirming the benefits of data-driven adaptation in exploiting the additional DoC provided by stacked physical architectures.

The study has been conducted under simplifying assump-

tions, including narrowband block-fading channels and single-carrier modulation. These limitations will be addressed in future work by leveraging the `ofdm` sub-module of `sionna` and the OpenNTN framework [28]. Future extensions include wideband channel modeling, robust learning under partial CSI, and online adaptation techniques tailored to time-varying NTN scenarios.

By introducing an open and scalable integration of SIM into an AI-native simulator, this work establishes a foundation for programmable, software-defined environments in next-generation aerospace and satellite communication systems.

ACKNOWLEDGEMENTS

This work was partially supported by the European Union-Next Generation EU under the Italian National Recovery and Resilience Plan (NRRP), Mission 4, Component 2, Investment 1.3, CUP E63C22002040007, partnership on “Telecommunications of the Future” (PE00000001 - program “RESTART”).

The work of I. Iudice was partially supported by the Italian National Project “Maturazione Tecnologie Innovative Mini e Micro Droni (MATIM)” through Programma Nazionale di Ricerche Aeroespaziali (PRORA) under Grant DM662.

The research activities presented in this paper fall within the field of interest of the IEEE AESS technical panel on Glue Technologies for Space Systems.

REFERENCES

- [1] K. B. Letaief, W. Chen, Y. Shi, J. Zhang, and Y.-J. A. Zhang, “The roadmap to 6G: AI empowered wireless networks,” *IEEE Communications Magazine*, vol. 57, no. 8, pp. 84–90, 2019.
- [2] C. Pan, H. Ren, K. Wang, J. F. Kolb, M. Elkashlan, M. Chen, M. Di Renzo, Y. Hao, J. Wang, A. L. Swindlehurst, X. You, and L. Hanzo, “Reconfigurable intelligent surfaces for 6G systems: Principles, applications, and research directions,” *IEEE Communications Magazine*, vol. 59, no. 6, pp. 14–20, 2021.
- [3] S. Basharat, S. A. Hassan, H. Pervaiz, A. Mahmood,

Z. Ding, and M. Gidlund, “Reconfigurable intelligent surfaces: Potentials, applications, and challenges for 6G wireless networks,” *IEEE Wireless Communications*, vol. 28, no. 6, pp. 184–191, 2021.

[4] C. E. Worka, F. A. Khan, Q. Z. Ahmed, P. Sureephong, and T. Alade, “Reconfigurable intelligent surface (RIS)-assisted non-terrestrial network (NTN)-based 6G communications: A contemporary survey,” *Sensors*, vol. 24, no. 21, 2024. [Online]. Available: <https://www.mdpi.com/1424-8220/24/21/6958>

[5] N. U. Hassan, J. An, M. Di Renzo, M. Debbah, and C. Yuen, “Efficient beamforming and radiation pattern control using stacked intelligent metasurfaces,” *IEEE Open Journal of the Communications Society*, vol. 5, pp. 599–611, 2024.

[6] M. Nerini and B. Clerckx, “Physically consistent modeling of stacked intelligent metasurfaces implemented with beyond diagonal ris,” *IEEE Communications Letters*, vol. 28, no. 7, pp. 1693–1697, 2024.

[7] J. An, C. Yuen, Y. L. Guan, M. D. Renzo, M. Debbah, H. V. Poor, and L. Hanzo, “Two-dimensional direction-of-arrival estimation using stacked intelligent metasurfaces,” *IEEE Journal on Selected Areas in Communications*, vol. 42, no. 10, pp. 2786–2802, 2024.

[8] J. An, C. Xu, D. W. K. Ng, G. C. Alexandropoulos, C. Huang, C. Yuen, and L. Hanzo, “Stacked intelligent metasurfaces for efficient holographic MIMO communications in 6g,” *IEEE Journal on Selected Areas in Communications*, vol. 41, no. 8, pp. 2380–2396, 2023.

[9] J. Hoydis, S. Cammerer, F. A. Aoudia, and *et al.*, “Sionna: An open-source library for next-generation physical layer research,” *arXiv preprint*, 2022.

[10] J. Hoydis, S. Cammerer, F. Aït Aoudia, M. Nimier-David, L. Maggi, G. Marcus, A. Vem, and A. Keller, “Sionna,” <https://github.com/NVlabs/sionna>, 2025, gPU-accelerated, differentiable 6G research library.

[11] J. Zhao, “A survey of intelligent reflecting surfaces (IRSs): Towards 6G wireless communication networks,” *arXiv preprint*, 2019.

[12] Y. Liu, X. Liu, X. Mu, T. Hou, J. Xu, M. Di Renzo, and N. Al-Dhahir, “Reconfigurable intelligent surfaces: Principles and opportunities,” *IEEE Communications Surveys & Tutorials*, vol. 23, no. 3, pp. 1546–1577, 2021.

[13] P. Putranto, A. A. Hamza, S. Mabrouki, N. Armi, and I. Dayoub, “Reconfigurable intelligent surfaces for 6G and beyond: A comprehensive survey,” *arXiv preprint*, 2025.

[14] A. Umer, I. Müürsepp, M. M. Alam, and H. Wymeersch, “Reconfigurable intelligent surfaces in 6G radio localization: A survey of recent developments, opportunities, and challenges,” *IEEE Communications Surveys & Tutorials*, pp. 1–1, 2025.

[15] Q. Wu and R. Zhang, “Towards smart and reconfigurable environment: Intelligent reflecting surface aided wireless network,” *IEEE Communications Magazine*, vol. 58, no. 1, pp. 106–112, 2020.

[16] NVIDIA Labs, “Sionna rt: Differentiable ray tracing for radio propagation modeling,” <https://nvlabs.github.io/sionna/>, 2023.

[17] X. Lin, Y. Rivenson, N. T. Yardimci, M. Veli, Y. Luo, M. Jarrahi, and A. Ozcan, “All-optical machine learning using diffractive deep neural networks,” *Science*, vol. 361, no. 6406, pp. 1004–1008, 2018. [Online]. Available: <https://www.science.org/doi/abs/10.1126/science.aat8084>

[18] C. Liu, Q. Ma, Z. J. Luo, Q. R. Hong, Q. Xiao, H. C. Zhang, L. Miao, W. M. Yu, Q. Cheng, L. Li *et al.*, “A programmable diffractive deep neural network based on a digital-coding metasurface array,” *Nature Electronics*, vol. 5, no. 2, pp. 113–122, 2022.

[19] J. An, M. Di Renzo, M. Debbah, and C. Yuen, “Stacked intelligent metasurfaces for multiuser beamforming in the wave domain,” in *ICC 2023 - IEEE International Conference on Communications*, 2023, pp. 2834–2839.

[20] H. Liu, J. An, D. W. K. Ng, G. C. Alexandropoulos, and L. Gan, “DRL-based orchestration of multi-user MISO systems with stacked intelligent metasurfaces,” in *ICC 2024 - IEEE International Conference on Communications*, 2024, pp. 4991–4996.

[21] X. Yao, J. An, L. Gan, M. Di Renzo, and C. Yuen, “Channel estimation for stacked intelligent metasurface-assisted wireless networks,” *IEEE Wireless Communications Letters*, vol. 13, no. 5, pp. 1349–1353, 2024.

[22] S. Lin, J. An, L. Gan, M. Debbah, and C. Yuen, “Stacked intelligent metasurface enabled LEO satellite communications relying on statistical CSI,” *IEEE Wireless Communications Letters*, vol. 13, no. 5, pp. 1295–1299, 2024.

[23] J. W. Goodman, *Introduction to Fourier optics*. Roberts and Company publishers, 2005.

[24] D. Darsena, F. Verde, I. Iudice, and V. Galdi, “Design of stacked intelligent metasurfaces with reconfigurable amplitude and phase for multiuser downlink beamforming,” *IEEE Open Journal of the Communications Society*, vol. 6, pp. 531–550, 2025.

[25] M. Joham, W. Utschick, and J. Nossek, “Linear transmit processing in MIMO communications systems,” *IEEE Transactions on Signal Processing*, vol. 53, pp. 2700–2712, Aug. 2005.

[26] C. R. Horn, R. A. & Johnson, *Matrix Analysis*. Cambridge University Press, Cambridge., 1985.

[27] F. Chollet *et al.*, “Keras,” <https://keras.io>, 2015.

[28] T. Düe, M. Vakilifard, C. Bockelmann, D. Wübben, and A. Dekorsy, “An open source channel emulator for non-terrestrial networks,” in *Advanced Satellite Multimedia Systems Conference/Signal Processing for Space Communications Workshop (ASMS/SPSC 2025)*, Sitges, Spain, Feb 2025. [Online]. Available: <https://www.ant.uni-bremen.de/sixcms/media.php/102/15080/An%20Open%20Source%20Channel%20Emulator%20for%20Non-Terrestrial%20Networks.pdf>



Ivan Iudice was born in Livorno, Italy, in 1986. He received the B.S. and M.S. degrees in telecommunications engineering in 2008 and 2010, respectively, and the Ph.D. degree in information technology and electrical engineering in 2017, all from University of Napoli Federico II, Italy. Since 2011, he has been with the Italian Aerospace Research Centre (CIRA), Capua, Italy. He first served as part of the Electronics and Communications Laboratory and he is currently part of the Security Unit. His research activities mainly lie in the area of signal and

array processing for communications, with current interests focused on physical-layer security, space-time techniques for cooperative communications systems and reconfigurable metasurfaces. He is involved in several international projects. He serves as reviewer for several international journals and as TPC member for several international conferences. He is author of several papers on refereed journals and international conferences. He has been serving as an Associate Editor for IEEE SIGNAL PROCESSING LETTERS since 2025.



Giacinto Gelli was born in Napoli, Italy, in 1964. He received the Dr. Eng. degree *summa cum laude* in electronic engineering in 1990, and the Ph.D. degree in computer science and electronic engineering in 1994, both from the University of Napoli Federico II, Italy. From 1994 to 1998, he was an Assistant Professor with the Department of Information Engineering, Second University of

Napoli, Italy. Since 1998 he has been with the Department of Electrical Engineering and Information Technology, University of Napoli Federico II, Italy, first as an Associate Professor, and since November 2006 as a Full Professor of Telecommunications. He also held teaching positions at the University Parthenope of Napoli, Italy and at the Accademia Aeronautica of Pozzuoli, Italy. His research interests are in the broad area of signal and array processing for communications, with current emphasis on multicarrier modulation systems, space-time techniques for cooperative and cognitive communications systems, and backscatter communications.



Donatella Darsena received the Dr. Eng. degree (summa cum laude) in telecommunications engineering and the Ph.D. degree in electronic and telecommunications engineering from the University of Napoli Federico II, Italy, in 2001 and 2005, respectively, where she is currently an Associate Professor with the Department of Electrical Engineering and Information Technology. From 2001 to 2002, she worked as an Embedded System Designer with the Telecommunications, Peripherals and Automotive Group, STMicroelectronics, Milano, Italy. In 2005, she joined the Department of Engineering, Parthenope University of Napoli, Italy, and worked first as an Assistant Professor and then as an Associate Professor from 2005 to 2022. Her research interests are in the broad area of signal processing for communications, with current emphasis on reflected-power communications, orthogonal and nonorthogonal multiple access techniques, wireless system optimization, and physical-layer security. She has served as a Senior Editor for IEEE ACCESS since 2024, as Executive Editor for IEEE COMMUNICATIONS LETTERS since 2023, and as Associate Editor for IEEE SIGNAL PROCESSING LETTERS since 2020. She was an Associate Editor for IEEE ACCESS from 2018 to 2023, and for IEEE COMMUNICATIONS LETTERS from 2016 to 2019, and a Senior Area Editor for IEEE COMMUNICATIONS LETTERS from 2020 to 2023.